How to cite: Angew. Chem. Int. Ed. 2023, e202311476
doi.org/10.1002/anie.202311476

VIP Biosensors Very Important Paper

Engineered Glucose Oxidase-Carbon Nanotube Conjugates for Tissue-Translatable Glucose Nanosensors

*Shoichi Nishitani, Tiffany Tran, Andrew Puglise, Sounghyun Yang, and Markita P. Landry**

Abstract: Continuous and non-invasive glucose monitoring and imaging is important for disease diagnosis, treatment, and management. However, glucose monitoring remains a technical challenge owing to the dearth of tissue-transparent glucose sensors. In this study, we present the development of near-infrared fluorescent single-walled carbon nanotube (SWCNT) based nanosensors directly functionalized with glucose oxidase (GOx) capable of immediate and reversible glucose imaging in biological fluids and tissues. We prepared GOx-SWCNT nanosensors by facile sonication of SWCNT with GOx in a manner that—surprisingly—does not compromise the ability of GOx to detect glucose. Importantly, we find by using denatured GOx that the fluorescence modulation of GOx-SWCNT is not associated with the catalytic oxidation of glucose but rather triggered by glucose-GOx binding. Leveraging the unique response mechanism of GOx-SWCNT nanosensors, we developed catalytically inactive apo-GOx-SWCNT that enables both sensitive and reversible glucose imaging, exhibiting a $\Delta F/F_0$ of up to 40 % within 1 s of exposure to glucose without consuming the glucose analyte. We finally demonstrate the potential applicability of apo-GOx-SWCNT in biomedical applications by glucose quantification in human plasma and glucose imaging in mouse brain slices.

[*] Prof. Dr. M. P. Landry
Department of Chemical and Biomolecular Engineering, University of California
94720 Berkeley, CA (USA)
and
Innovative Genomics Institute (IGI)
94720 Berkeley, CA (USA)
and
California Institute for Quantitative Biosciences, QB3, University of California
94720 Berkeley, CA (USA)
and
Chan-Zuckerberg Biohub
94158 San Francisco, CA (USA)
E-mail: landry@berkeley.edu
Dr. S. Nishitani, T. Tran, A. Puglise, S. Yang
Department of Chemical and Biomolecular Engineering, University of California
94720 Berkeley, CA (USA)

Introduction

Glucose, as a vital energy source in living organisms, plays a crucial role in various physiological processes. Therefore, precise regulation of glucose levels is essential, and abnormal glucose metabolism has been associated with a range of diseases, including diabetes, neurodegeneration, and cancer.[1,2] Consequently, the development of tissue-transparent glucose nanosensors holds significant potential for disease diagnosis, treatment, and management. Electrochemical sensors traditionally employ glucose oxidase (GOx), a glucose-specific oxidative enzyme, as the gold standard for blood glucose tests in diabetes management.[3] However, direct in-body or in-tissue glucose detection using electrochemical readouts faces technical challenges due to the use of electronic circuits which can be bulky and require batteries. Additionally, the enzymatic activity of native GOx compromises the reversibility of the sensors, rendering them unsuitable for continuous glucose sensing and imaging applications.

In this context, single-walled carbon nanotubes (SWCNTs) are promising bioimaging candidates that may enable tissue-translatable glucose detection and imaging due to their attractive optical properties such as intrinsic fluorescence emission in the near-infrared (nIR) and their non-photobleaching nature.[4–6] Furthermore, the fluorescence properties of SWCNTs can be modulated by the surrounding environment.[7] For example, SWCNTs conjugated to certain ssDNA sequences show strong turn-on fluorescence modulation upon exposure to neurotransmitters, such as dopamine and other catecholamines.[8] SWCNT-based nanosensors can also be evolved to exhibit molecular recognition for specific analytes, though this evolution of synthetic molecular recognition has not yet been shown to work for protein recognition.[9] On the other hand, proteins are another class of biomolecules that can be conjugated to SWCNTs.[10–13] Owing to their substrate-specific enzymatic activity, enzymes can be used to rationally design nanosensors for a specific analyte of interest.[14] Taking advantage of these attractive properties of SWCNTs and specifically the glucose recognizability of GOx, several SWCNT-based glucose nanosensors have been reported, with challenges including low synthesis scalability, sub-par colloidal stability, and poor reversibility.[7,15–18]

The synthesis of SWCNT-based nanosensors via biomolecule-SWCNT conjugation is typically accomplished through ultrasonication of polymer-SWCNT conjugates or through dialysis-based ligand exchange of biomolecule-SWCNT conjugates.[5,19] While probe tip sonication is quick

and high-yielding, this method is typically deemed unsuitable for protein-SWCNT conjugation due to the denaturation of proteins under the high shear stresses induced by probe tip sonication.[11,20] While certain proteins like serum albumin have successfully dispersed SWCNT with probe tip sonication at the expense of protein integrity, proteins such as GOx were previously found not to suspend SWCNT in an aqueous solution.[21,22] Owing to the high relevance of SWCNT-based sensors and their near-infrared tissue-transparent fluorescence, SWCNT-based glucose sensors have previously been prepared with dialysis-based ligand exchange, which remains the only technique for generating GOx-SWCNT conjugates for glucose sensing, although the procedure is not optimal due to the low yield and poor colloidal stability of the resulting nanosensors. This low colloidal stability precludes direct glucose imaging in biologically relevant biofluids and tissues[7,17]

In the present study, we hypothesize that GOx can be directly conjugated to SWCNT through direct probe tip sonication under optimal sonication and GOx:SWCNT mass ratio conditions to generate enzyme-SWCNT-based nanosensors for sensing and imaging applications. We show that with optimized conditions, GOx-SWCNT conjugates can be prepared by sonication with appreciable yield and glucose sensing ability. Next, we investigate the mechanism of fluorescence modulation using denatured GOx, showing that the enzyme's catalytic reaction counterintuitively does not cause fluorescence modulation, instead attributing GOx-SWCNT nanosensors' responses to a glucose-enzyme binding. This result motivated us to develop sensitive and reversible nanosensors by synthesizing apo-GOx, nanosensors generated from bioengineered GOx, showing their potential applicability in tissue-translatable glucose sensing and imaging.

Results and Discussion

Facile generation and characterization of GOx-nanotube based nanosensors

We synthesized GOx-SWCNT nanosensors via direct sonication of SWCNT with GOx. The strong shear-force generated by the tip sonicator continuously unbundles SWCNTs in the solution, facilitating protein adsorption to SWCNT surfaces and suspending individual nanotubes in an aqueous solution (Figure 1a). We purified the synthesized nanosensors via centrifugation and dialysis. In contrast to previous reports that GOx cannot suspend SWCNTs, we identified optimal enzyme:SWCNT mass ratio and sonication strength parameters for successfully generating GOx-SWCNT conjugates (Supporting Information S1).[21] The suspensions synthesized via this method exhibited a high yield of 20 mg/L, and excellent colloidal stability for several months without forming any aggregations, unlike those generated through dialysis-based ligand exchange. Atomic

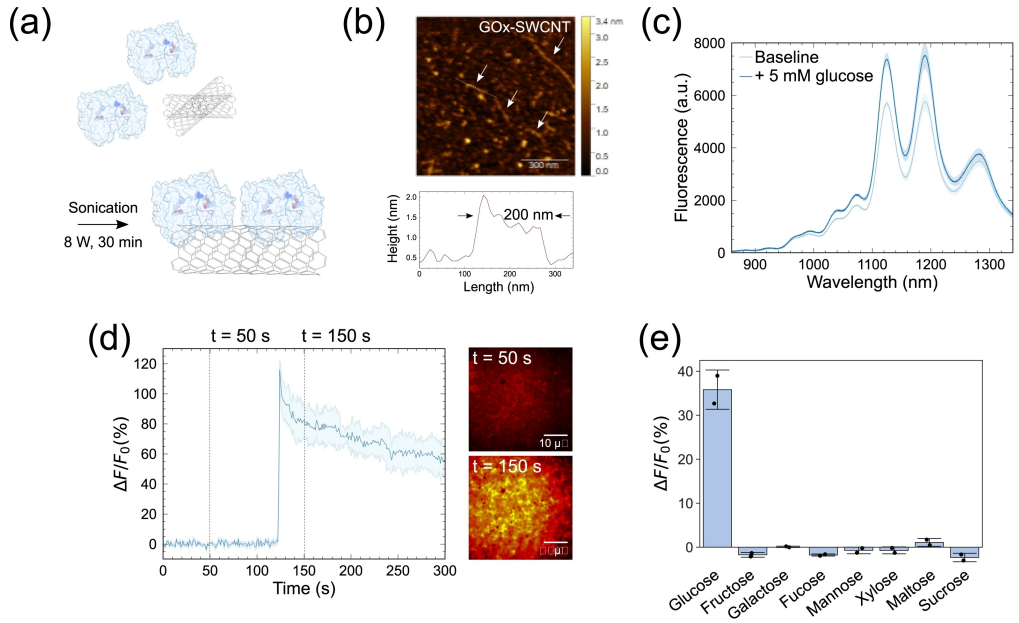

Figure 1. Generation and characterization of GOx-SWCNT-based glucose nanosensors. (a) Schematic illustration of sonication-based physisorption of enzymes to SWCNT. (b) An AFM image of immobilized nanosensors on a mica substrate (top) with representative height profile of an individual nanosensor (bottom). Arrows point to individual nanotubes. (c) Average trace of the fluorescence emission spectra of the nanosensors before (light blue) and immediately after (blue) exposure to 5 mM glucose ($N=2$), with the colored area representing the standard deviation. (d) Average $\Delta F/F_0$ trace of immobilized GOx-SWCNT nanosensors. PBS was added at 60 s, and 10 mM glucose was added at 120 s. Average $\Delta F/F_0$ was calculated from ten randomly selected nanosensors, with the area representing standard deviation. Representative images before (t = 50 s) and after (t = 150 s) glucose addition are shown on the right. (e) Peak solution-phase $\Delta F/F_0$ responses at the (7,6) chirality of GOx-SWCNT nanosensors 20 min after exposure to 5 mM of glucose and analogs: Fructose, Galactose, Fucose, Mannose, Xylose, Maltose, and Sucrose ($N=2$), with error bars representing standard deviation.

force microscopy (AFM) imaging confirmed individually-suspended and uniformly dispersed GOx-SWCNTs (Figure 1b), with average lengths and heights of 270 ± 77 nm and 0.93 ± 0.13 nm, respectively, consistent with the dimensions of SWCNTs. Furthermore, GOx almost entirely occupied the surface of the SWCNT, suggesting the formation of a dense GOx monolayer on the SWCNT surface and potentially contributing to the colloidal stability of the nanosensors (Supporting Information S2).

Next, we examined the nIR fluorescence responsivity of GOx-SWCNT nanosensors to different glucose concentrations in phosphate-buffered saline (PBS). The fluorescence intensity of the nanosensors increased immediately upon exposure to glucose, indicating that direct sonication of GOx with SWCNTs—surprisingly—did not compromise the ability of the GOx to detect glucose (Figure 1c). Specifically, in solution, the GOx-SWCNT nanosensor $\Delta F/F_0$ (change in fluorescence intensity normalized to the baseline fluorescence) reached 40 % upon the addition of 5 mM glucose at the (7,6) chiral peak ($\lambda_{em} = 1194$ nm). This in solution response is comparable to that of nanosensors prepared by a dialysis-based ligand exchange method.[17] Moreover, the surface-immobilized nanosensor response to glucose was instantaneous and reached a $\Delta F/F_0 = 100\,\%$, reaching this maximum $\Delta F/F_0$ within one second after glucose exposure (Figure 1d). To confirm the role of physisorbed GOx on fluorescence responses, we compared the response of GOx-SWCNT nanosensors with two controls: GOx-SWCNT prepared via probe tip sonication, but they were subject to dialysis to remove any GOx not bound to the SWCNT surface, and BSA-SWCNT prepared via sonication (Figure S2). Dialyzed GOx-SWCNT retained the nanosensor response to glucose, as expected, whereas BSA-SWCNT did not respond to glucose, also as expected, confirming that the glucose-specific activity of surface-bound GOx generates the fluorescence modulation of the nanosensors. We next confirmed the selectivity of the nanosensors by testing the flurescence modulation of GOx-SWCNT to various saccharide analogs: Fructose, Galactose, Fucose, Mannose, Xylose, Maltose, Sucrose. We find that equimolar concentrations of these saccharides cause no fluorescence modulation of GOx-SWCNT, indicating that GOx-SWCNT nanosensors only responded to glucose and confirming the structural selectivity of the enzyme after adsorption to SWCNTs (Figure 1e). These findings demonstrate the successful generation of glucose nanosensors using the direct sonication methodology.

Catalytically inactive nanosensors reveal an affinity-based modulation mechanism

We next studied the mechanism behind the fluorescence modulation of GOx-SWCNT-based nanosensors. We hypothesized that GOx-SWCNT nanosensor responses could either be the result of catalytic oxidation of glucose, as previously proposed,[17] or by glucose binding but without catalytic oxidation (see Supporting Information S3 for details). Previously, Zubkovs et al. synthesized GOx-SWCNT via a ligand exchange approach and proposed a theoretical fluorescence response mechanism involving catalytic redox reactions, where electrons transferred from glucose to the enzyme passivate the p-doped oxygen sites, thereby increasing the fluorescence emission.[17] To investigate whether the catalytic activity of GOx is necessary for the fluorescence modulation of GOx-SWCNT nanosensors, we irreversibly deactivated GOx and prepared catalytically inactive nanosensors. Heating above the transition temperature of 56 °C irreversibly denatures GOx, which also releases the cofactor flavine adenine dinucleotide (FAD) from the enzyme.[23] This thermal denaturation completely deactivates the catalytic activity of GOx. Notably, GOx is a unique type of enzyme known to maintain its dimeric and globule-like apoenzyme structures after denaturation.[24] Therefore, we hypothesized that dGOx preserves the glucose-binding cavity and can thus be utilized to verify whether the GOx-SWCNT nanosensor fluorescence modulation is induced by an enzymatic reaction or by substrate-enzyme binding.

GOx was denatured by heating it to 65 °C for 15 min in 10 mM phosphate buffer at pH 5.5 (Figure 2a). To confirm the release of FAD from the enzyme, we dialyzed dGOx in the same buffer for 24 hours. After dialysis, the yellow color of FAD disappeared, and the solution became colorless, confirming the release of FAD from the GOx enzyme (photo in Figure S5). We confirmed the complete loss of activity of dGOx (0.05 % enzymatic activity relative to the native GOx) using a commercially available fluorescence-based activity assay (Figure S5). Furthermore, dGOx remained inactive even after re-incubation in FAD for 12 h (0.03 % enzymatic activity relative to the native GOx).

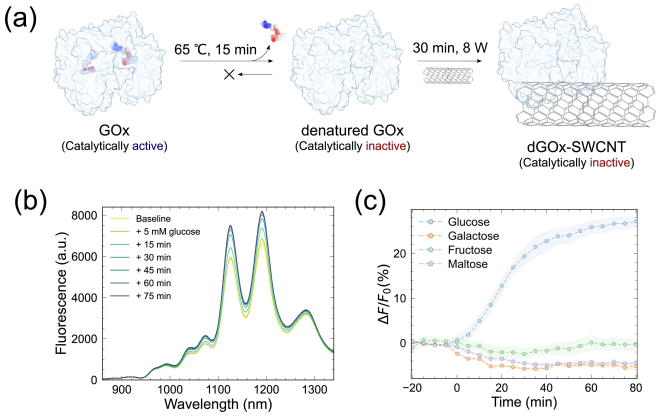

Figure 2. Generation of catalytically inactive glucose nanosensors by using thermally denatured GOx, and investigation of modulation mechanism. (a) Schematic representation of irreversible GOx denaturation and corresponding dGOx-SWCNT generation. (b) Time-dependent average fluorescence emission spectra of the dGOx-SWCNT before and after exposure to 5 mM glucose, with the area showing standard deviation ($N = 2$). (c) The average $\Delta F/F_0$ traces at the (7,6) chirality of the dGOx-SWCNT nanosensors upon addition of 5 mM glucose (blue), galactose (orange), fructose (green), and maltose (purple). Analytes were added at 0 min. ($N = 2$, colored area represents standard deviation.)

Therefore, we confirmed that GOx was irreversibly deactivated by thermal denaturation.

Next, we proceeded to synthesize dGOx-SWCNT conjugates and characterized their nIR fluorescence responses. We applied the same synthesis procedure and conditions as we did for the GOx-SWCNT synthesis (Figure 2a). Surprisingly, the loss of catalytic activity did not impair the ability of the nanosensors to detect glucose, albeit with a nanosensor turn-on response that was not immediate. The fluorescence intensity of the catalytically inactive dGOx-SWCNT increased after exposure to glucose (Figure 2b). The $\Delta F/F_0$ increased gradually following exposure to 5 mM glucose, reaching a maximum of 30 % within 1 hour (Figure 2b and 2c), which is comparable to the response of GOx-SWCNT. Moreover, deactivation did not affect the selectivity of glucose detection, as exposing the nanosensors to the same concentration of galactose and other saccharide analogs resulted in negligible nanosensor fluorescence intensity changes (Figure 2c). These results clearly demonstrate that the fluorescence modulation of GOx-SWCNT is not associated with the catalytic oxidation of glucose but rather predominately triggered by substrate-enzyme binding, though not completely eliminating the contribution of redox processes, as also suggested by the fluorescence intensity changes.[25] These findings are particularly important for real-time glucose quantification or tissue imaging, as the consumption of the analyte changes the analyte local concentration and thus compromises the reversibility of the nanosensors. Moreover, the use of inactive GOx enables nanosensors to detect glucose without generating toxic H_2O_2 as a byproduct. In this regard, deactivated enzymes may enable the generation of reversible and biocompatible nanosensors for enzyme-substrate pairs other than GOx/glucose and for sensing modalities beyond SWCNT.

We examined the catalytically inactive nature of the deactivated nanosensors by comparing the time-dependent $\Delta F/F_0$ responses of the catalytically active (GOx-SWCNT) and inactive (dGOx-SWCNT) nanosensors for various glucose concentrations. As expected, the active nanosensors showed an immediate increase in $\Delta F/F_0$ upon exposure to all tested concentrations of glucose, which gradually decreased over time due to continuous glucose consumption (Figure 3a). In contrast, dGOx-SWCNT exhibited a stable $\Delta F/F_0$ response over the measurement period, demonstrating the reliability of inactive nanosensors for continuous glucose measurement without affecting local concentrations of the substrate. However, one drawback of denaturation was the compromised affinity of the nanosensors, as evidenced by the increased response time. Figure 3c shows the dose-based response curves of GOx-SWCNT and dGOx-SWCNT nanosensors, with the response curve inflection of dGOx-SWCNT shifting horizontally towards a higher concentration range than its enzymatically-active counterpart, indicating the lower binding affinity of glucose-dGOx-SWCNT compared to glucose-GOx-SWCNT. To quantify the difference in binding affinity, we applied the Hill equation to fit the response curve to extract the dissociation constant, K_d. Since glucose-GOx affinity-based binding determines the nanosensor $\Delta F/F_0$ response, we chose the Hill equation derived

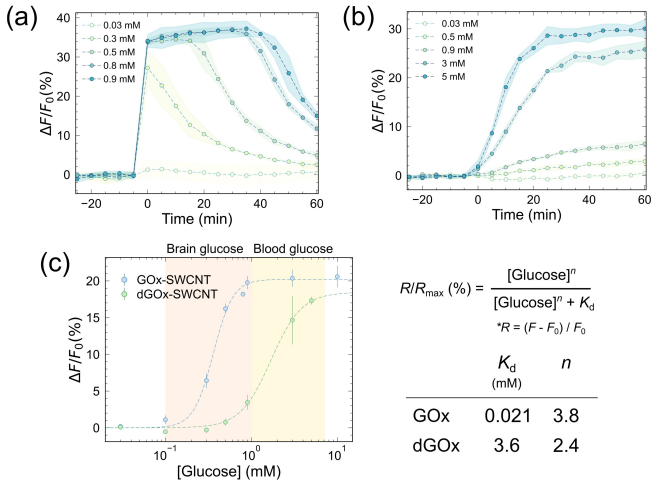

Figure 3. Time-dependent response of dGOx-SWCNT nanosensors and their compromised affinity to glucose. Time-dependent $\Delta F/F_0$ traces at the (7,6) chirality of GOx-SWCNT ($N=3$) (a) and dGOx-SWCNT ($N=4$) (b) upon exposure to various concentrations of glucose. Glucose was added at 0 min. The colored area represents standard deviation. (c) The dose-based response curves of GOx-SWCNT (orange) and dGOx-SWCNT (purple) nanosensors, fitted by the Hill equation as shown on the right (fitted lines represented by the dashed lines) The extracted values are listed on the right table ($N=2$, error bars show standard deviation). Maximum $\Delta F/F_0$ values were used to draw the response curves. Nanosensors were dialyzed prior to the measurement. The colored region represents the physiological glucose concentrations in the brain (pink) and blood (yellow).

from substrate-receptor binding systems to fit the data. Consequently, the K_d of dGOx-SWCNT was found to be 170 times larger than that of GOx-SWCNT, as expected since denaturation alters the structure of GOx to some extent. The shaded region in Figure 3c represents physiologically-relevant glucose concentrations in the brain and blood. While dGOx-SWCNT is suitable for glucose detection in blood, high-affinity GOx-SWCNT is required for detecting glucose in the brain.[26] Therefore, the development of both sensitive and reversible nanosensors are ideal for glucose imaging in the brain.

Engineered GOx enables generation of sensitive and catalytically inactive nanosensors for glucose sensing and imaging in biological systems

Deactivation of GOx allows generation of reversible glucose nanosensors, yet it compromises glucose-GOx binding affinity, sacrificing the sensitivity and response time of the nanosensors. Based on these observations, we hypothesized that deactivating GOx while minimizing the structural alteration of the enzyme could enable the generation of reversible *and* sensitive nanosensors. To test this hypothesis, we prepared an apo form of GOx (apo-GOx) by removing FAD from GOx, as depicted in Figure 4a. While denaturation is associated with irreversible deflavination, deflavination to produce apo-GOx is reversible. As such, we expect apo-GOx to better preserve the native structure of GOx

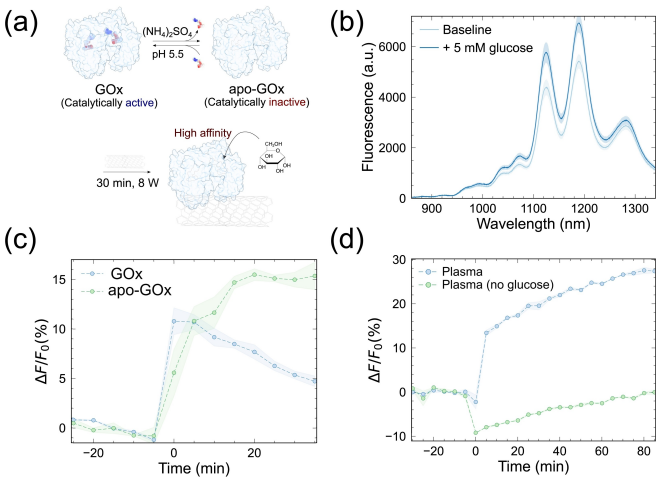

Figure 4. Generation and characterization of apo-GOx-SWCNT based glucose nanosensors. (a) Schematic illustration of apo-GOx and corresponding nanosensor generation. (b) Average traces of the nIR fluorescence emission spectra of apo-GOx-SWCNT before (light blue) and immediately after (blue) exposure to 5 mM glucose. (c) Time-dependent $\Delta F/F_0$ traces at the (7,6) chirality of GOx-SWCNT (blue) and aGOx-SWCNT (green, $N=4$) upon exposure to 500 μM glucose. Glucose was added at 0 min. Nanosensors were dialyzed prior to the measurement (d) Average $\Delta F/F_0$ traces at the (7,6) chirality of apo-GOx-SWCNT upon exposure to human plasma (blue, 10 μL whole plasma was added to 90 μL nanosensor solution). For the control (green), plasma was digested with GOx. $N=2$ for all data unless stated individually, and the colored area represents standard deviation.

compared to dGOx. In fact, previous studies have demonstrated that catalytically inactive apo-GOx has a glucose binding affinity comparable to that of the native form of GOx.[27,28] These properties of apo-GOx motivated us to develop apo-GOx-based nanosensors (apo-GOx-SWCNT) that allow for reliable and sensitive glucose detection with tissue transparency.

To obtain apo-GOx, we removed FAD from GOx by precipitating it in a saturated ammonium sulfate solution that was acidified to pH 1.4, as illustrated in Figure 4a.[29] We harvested the resulting apo pellets by centrifugation and then resuspended them in 2.5 M sodium acetate (pH 8.5). Finally, the apo solution was dialyzed in 10 mM phosphate buffer (pH 6.8) to obtain a clear, colorless solution. We confirmed the complete deactivation of apo-GOx using the GOx activity assay (blue and green traces in Figure S6). Furthermore, we found that apo-GOx could be reactivated by incubating with FAD for 2 hours, with an efficiency of up to 80 %, thus demonstrating the superiority of apo-GOx from irreversibly denatured GOx in terms of the stability of their structural integrity (purple trace in Figure S6).

Next, we synthesized apo-GOx-SWCNT conjugates using the same above-mentioned probe tip sonication protocol. As shown in Figure 4b, the nIR fluorescence emission spectra of apo-GOx-SWCNT increased immediately upon exposure to 5 mM glucose, consistent with our hypothesis. The maximum $\Delta F/F_0$ reached 40 %, indicating that apo-GOx-SWCNT generates a response to glucose similar to GOx-SWCNT. Furthermore, apo-GOx-SWCNT exhibited a response time comparable to that of GOx-SWCNT and was faster than that of dGOx-SWCNT, indicating that apo-GOx has a markedly higher binding affinity to glucose than that of dGOx (Figure S7 and 4c). Comparing dose-based response curves further provided evidence that apo-GOx-SWCNT exhibits similar sensitivity characteristics to native GOx-SWCNT (Figure S8). Accordingly, apo-GOx-SWCNT had a dynamic range between 0.1 mM and 3 mM, and the limit of detection (LOD), determined as blank response + 3σ, was 42 μM. This dynamic range covers physiologically-relevant concentrations of glucose, particularly in the brain (Figure 3c), and LOD is sufficiently low to detect glucose levels as low as 100 μM in hypoglycemic conditions. Moreover, continuous monitoring of fluorescence emission at 500 μM glucose revealed an expected catalytically inactive nature of apo-GOx-SWCNT similar to dGOx-SWCNT (Figure 4c). While GOx-SWCNT and apo-GOx-SWCNT both responded instantaneously to the addition of glucose, apo-GOx-SWCNT maintained a stable fluorescence response, whereas the fluorescence emission of GOx-SWCNT continuously decreased due to glucose consumption. Reversibility of the fluorescence response was separately confirmed by a dialysis-based measurement setup (Figure S10). Furthermore, we confirmed that apo-GOx-SWCNT generates a negligible amount of H_2O_2 compared to H_2O_2 generated with GOx-SWCNT. As discussed previously, this feature minimizes nanosensor toxicity, and thus motivates in vivo applications of apo-GOx-SWCNT nanosensors. Finally, we confirmed that the structural integrity of apo-GOx-SWCNT is maintained by testing the nanosensor response to glucose analogs, in which the nanosensor generated negligible responses to all analytes except for glucose (Figure S11). Consequently, we successfully synthesized reversible apo-GOx-SWCNT based glucose nanosensors that perform remarkably similar to those based on native GOx.

To investigate the applicability of apo-GOx-SWCNT as tissue translatable nanosensors for glucose monitoring, we evaluated the performance of these nanosensors in human serum and plasma. Remarkably, apo-GOx-SWCNT exhibited appreciable stability in serum and could generate a response to 5 mM of exogenously added glucose even after incubation for up to 3 days in whole serum (Figure S12). Next, we assessed the ability of apo-GOx-SWCNT to quantify glucose levels in human plasma. The biocompatibility of SWCNT-based nanosensors is often compromised in plasma because it contains fibrinogen, a protein well-known to have a strong affinity to SWCNT surfaces.[30] A control plasma sample without glucose was prepared by digesting glucose through plasma incubation with GOx. As opposed to the negligible fluorescence changes observed upon exposure to digested plasma, adding native plasma (which includes endogenous glucose) increased fluorescence intensity, indicating the nanosensors' ability to detect endogenous glucose in human plasma (Figure 4d). Using the above-mentioned Hill parameters, we estimated the glucose concentration in the human plasma sample to be 7 mM, which is consistent with the concentration of glucose levels expected in human plasma. We hypothesize that the high-density coverage of apo-GOx on SWCNT contributed to the

stability of nanosensors in human biofluid samples. We highlight that SWCNT-based nanosensors prepared by ssDNA, such as a $(GT)_6$-SWCNT dopamine nanosensor, lose their ability to detect their analyte, dopamine, immediately after exposure to 0.1X serum or plasma (Figure S13)—thus making glucose detection in both serum and plasma by apo-GOx quite remarkable. These findings demonstrate the potential of apo-GOx-SWCNT for non-invasive, continuous glucose quantification in biological fluids such as blood and dermal interstitial fluid.

Finally, we demonstrate the potential applicability of apo-GOx-SWCNT for real-time glucose imaging in biological tissues. SWCNT-based nanosensors have attractive properties suitable for tissue imaging, such as high spatiotemporal resolution, non-photobleaching nature, and fluorescence in the tissue-transmissive nIR region. Additionally, such imaging probes should possess reversibility for accurately quantifying analyte levels in biological specimens without consuming the substrate. To test the feasibility of using apo-GOx-SWCNT for glucose imaging in biological tissues, we used brain tissue from mice as a model tissue system. Glucose is the primary energy source for the brain and plays an essential role in neuronal activity. Disruptions to glucose metabolism homeostasis, such as hyperglycemia and hypoglycemia, have been linked to various pathologies, including cognitive impairment, dementia, Alzheimer's Disease, Parkinson's Disease, Huntington's Disease, and epilepsy.[31] Therefore, quantifying spatiotemporal changes in local changes in glucose consumption in the brain may lead to a better understanding of the diseases and potentially contribute to the development of therapeutics.

An acute coronal brain slice of 300 μm thickness was extracted from an adult black 6 mouse. We then labeled the extracted brain slice with apo-GOx-SWCNT by directly spraying the nanosensor solution onto the tissue slice surface, and the fluorescence emission of the immobilized nanosensors was imaged with an inverted near-infrared epifluorescence microscope (Figure 5a). As shown in Figure 5b and S14, surface adsorbed, individual nanosensors were successfully resolved in brain slices. The fluorescence intensity of surface adsorbed nanosensors increased rapidly upon exposure to 50 mM glucose that was introduced at 120 s, with $\Delta F/F_0$ reaching 40 % at maximum (Figure 5b and 5c). On the other hand, there was no marked increase in fluorescence when the same volume of phosphate buffer was added (Figure 5c and S14), demonstrating that immobilized apo-GOx-SWCNT are able to respond to the addition of exogenously added glucose with high spatiotemporal resolution. This illustrates the promise of apo-GOx-SWCNTs in investigating the variety of diseases and conditions that are associated with disturbances in glucose homeostasis in the brain, and more broadly confirms the unperturbed function of apo-GOx-SWCNT glucose nanosensors to image glucose in dense biological tissues.

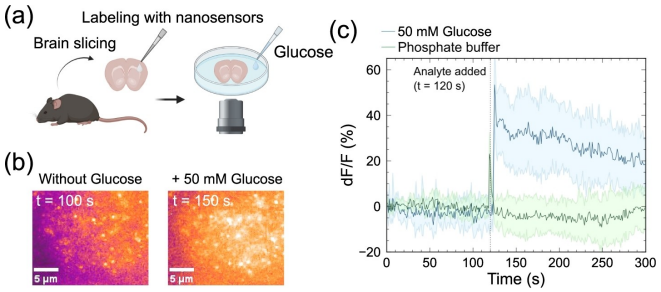

Figure 5. Imaging exogenous glucose in mouse brain tissue. (a) Schematic illustration of the experimental procedures. (b) Representative images of the immobilized nanosensors taken at 100 s (before exposure) and 150 s (after exposure to glucose). (c) Average trace of $\Delta F/F_0$ responses of brain slice-immobilized apo-GOx-SWCNT upon exposure to 50 mM glucose or phosphate buffer (control) over the time course of 300 s. The analyte was added at 120 s. $\Delta F/F_0$ was calculated from 10 randomly selected ROIs with the colored area representing standard deviation.

Conclusion

In this study, we developed a catalytically inactive apo-GOx-SWCNT for reversible glucose imaging and sensing applications. We first demonstrated that, counter to current undertanding, GOx-SWCNT conjugates can be prepared by direct probe-based sonication strategies that do not compromise the ability of the nanosensors to detect glucose. Next, we investigated the mechanism of GOx-SWCNT fluorescence modulation. By generating denatured GOx, we found that neither the enzymatic reaction nor its by-products are involved in SWCNT fluorescence modulation. Rather, glucose binding to GOx itself is the dominant cause of nanosensor fluorescence modulation. This finding is important because the enzymatic activity of the enzymes often compromises the environmental reversibility of the sensors, and undesirably consumes the analyte from which the measurements are being taken. With the reduced affinity of the denaturation, we hypothesized that both sensitive and reversible nanosensors can be prepared by deactivating the GOx enzyme with minimal structural alteration to the enzyme, which was achieved by synthesizing an apo-form of GOx. By using apo-GOx to generate glucose nanosensors by the same above-mentioned protocol, we developed reversible glucose nanosensors that also have appreciably similar responsivity to that of GOx-SWCNT. We then showed the potential applicability of these nanosensors for biosensing and imaging applications by applying them to the quantification of glucose levels in human plasma and exogenous glucose imaging in mouse brain slices. Our work herein both generates a tissue-translatable glucose nanosensor and motivates direct sonication and enzyme-SWCNT physisorption as a generalizable method for protein-based nanosensor generation.

Supporting Information

The authors have cited additional references within the Supporting Information.[31–34]

Acknowledgements

We acknowledge support of a Burroughs Wellcome Fund Career Award at the Scientific Interface (CASI) (MPL), a Dreyfus foundation award (MPL), the Philomathia foundation (MPL), an NIH MIRA award R35GM128922 (MPL), an NIH R21 NIDA award 1R03DA052810 (MPL), an NSF CAREER award 2046159 (MPL), an NSF CBET award 1733575 (to MPL), a CZI imaging award (MPL), a Sloan Foundation Award (MPL), a USDA BBT EAGER award (MPL), a Moore Foundation Award (MPL), a Schmidt Science Award (MPL), and a DOE office of Science grant DE-SC0020366 (MPL). MPL is a Chan Zuckerberg Biohub investigator and a Hellen Wills Neuroscience Institute Investigator.

Conflict of Interest

The authors declare no conflict of interest.

Data Availability Statement

The data that support the findings of this study are available in the supplementary material of this article.

Keywords: Biosensors · Imaging Agents · Single-Walled Carbon Nanotubes · Glucose · Glucose Oxidase

[1] T. A. Chowdhury, *QJM* **2010**, *103*, 905–915.
[2] M. A. Daulatzai, *J. Neurosci. Res.* **2017**, *95*, 943–972.
[3] S. J. Updike, G. P. Hicks, *Nature* **1967**, *214*, 986–988.
[4] Z. Liu, S. Tabakman, K. Welsher, H. Dai, *Nano Res.* **2009**, *2*, 85–120.
[5] M. J. O'Connell, S. M. Bachilo, C. B. Huffman, V. C. Moore, M. S. Strano, E. H. Haroz, K. L. Rialon, P. J. Boul, W. H. Noon, C. Kittrell, J. Ma, R. H. Hauge, R. B. Weisman, R. E. Smalley, *Science* **2002**, *297*, 593–596.
[6] J. V. Frangioni, *Curr. Opin. Chem. Biol.* **2003**, *7*, 626–634.
[7] P. W. Barone, S. Baik, D. A. Heller, M. S. Strano, *Nat. Mater.* **2005**, *4*, 86–92.
[8] S. Kruss, M. P. Landry, E. Vander Ende, B. M. A. Lima, N. F. Reuel, J. Zhang, J. Nelson, B. Mu, A. Hilmer, M. Strano, *J. Am. Chem. Soc.* **2014**, *136*, 713–724.
[9] S. Jeong, D. Yang, A. G. Beyene, J. T. Del Bonis-O'Donnell, A. M. M. Gest, N. Navarro, X. Sun, M. P. Landry, *Sci. Adv.* **2019**, *5*, eaay3771.
[10] S. S. Karajanagi, H. Yang, P. Asuri, E. Sellitto, J. S. Dordick, R. S. Kane, *Langmuir* **2006**, *22*, 1392–1395.
[11] S. S. Karajanagi, A. A. Vertegel, R. S. Kane, J. S. Dordick, *Langmuir* **2004**, *20*, 11594–11599.
[12] K. Matsuura, T. Saito, T. Okazaki, S. Ohshima, M. Yumura, S. Iijima, *Chem. Phys. Lett.* **2006**, *429*, 497–502.
[13] W. Feng, P. Ji, *Biotechnol. Adv.* **2011**, *29*, 889–895.
[14] R. Wilson, A. P. F. Turner, *Biosens. Bioelectron.* **1992**, *7*, 165–185.
[15] K. Yum, T. P. McNicholas, B. Mu, M. S. Strano, *J. Diabetes Sci. Technol.* **2013**, *7*, 72–87.
[16] P. W. Barone, R. S. Parker, M. S. Strano, *Anal. Chem.* **2005**, *77*, 7556–7562.
[17] V. Zubkovs, N. Schuergers, B. Lambert, E. Ahunbay, A. A. Boghossian, *Small* **2017**, *13*, 1701654.
[18] V. Zubkovs, H. Wang, N. Schuergers, A. Weninger, A. Glieder, S. Cattaneo, A. A. Boghossian, *Nanoscale Adv.* **2022**, *4*, 2420–2427.
[19] M. Zheng, A. Jagota, E. D. Semke, B. A. Diner, R. S. McLean, S. R. Lustig, R. E. Richardson, N. G. Tassi, *Nat. Mater.* **2003**, *2*, 338–342.
[20] S. Marchesan, M. Prato, *Chem. Commun.* **2015**, *51*, 4347–4359.
[21] D. Nepal, K. E. Geckeler, *Small* **2007**, *3*, 1259–1265.
[22] M. Calvaresi, F. Zerbetto, *Acc. Chem. Res.* **2013**, *46*, 2454–2463.
[23] M. D. Gouda, S. A. Singh, A. G. A. Rao, M. S. Thakur, N. G. Karanth, *J. Biol. Chem.* **2003**, *278*, 24324–24333.
[24] G. Zoldák, A. Zubrik, A. Musatov, M. Stupák, E. Sedlák, *J. Biol. Chem.* **2004**, *279*, 47601–47609.
[25] D. A. Heller, G. W. Pratt, J. Zhang, N. Nair, A. J. Hansborough, A. A. Boghossian, N. F. Reuel, P. W. Barone, M. S. Strano, *Proc. Natl. Acad. Sci. USA* **2011**, *108*, 8544–8549.
[26] A. Agrawal, G. Pekkurnaz, E. F. Koslover, *eLife* **2018**, *7*, https://doi.org/10.7554/eLife.40986.
[27] S. D'Auria, P. Herman, M. Rossi, J. R. Lakowicz, *Biochem. Biophys. Res. Commun.* **1999**, *263*, 550–553.
[28] K. Sugawara, N. Kamiya, G. Hirabayashi, H. Kuramitz, *Electroanalysis* **2006**, *18*, 1001–1006.
[29] K. Garajová, M. Zimmermann, M. Petrenčáková, L. Dzurová, M. Nemergut, Ľ. Škultéty, G. Žoldák, E. Sedlák, *Biophys. Chem.* **2017**, *230*, 74–83.
[30] R. L. Pinals, D. Yang, A. Lui, W. Cao, M. P. Landry, *J. Am. Chem. Soc.* **2020**, *142*, 1254–1264.
[31] E. Blázquez, V. Hurtado-Carneiro, Y. LeBaut-Ayuso, E. Velázquez, L. García-García, F. Gómez-Oliver, J. M. Ruiz-Albusac, J. Ávila, M. Á. Pozo, *Front. Endocrinol.* **2022**, *13*, 873301.
[32] L. S. Shlyakhtenko, A. A. Gall, Y. L. Lyubchenko, *Methods Mol. Biol.* **2013**, *931*, 295–312.
[33] S. J. Yang, J. T. Del Bonis-O'Donnell, A. G. Beyene, M. P. Landry, *Nat. Protoc.* **2021**, *16*, 3026–3048.
[34] Y. Wang, R. Jonkute, H. Lindmark, J. D. Keighron, A.-S. Cans, *Langmuir* **2020**, *36*, 37–46.

Manuscript received: August 7, 2023
Accepted manuscript online: November 21, 2023
Version of record online: ■■, ■■

Research Articles

Biosensors

S. Nishitani, T. Tran, A. Puglise, S. Yang, M. P. Landry* ——— **e202311476**

Engineered Glucose Oxidase-Carbon Nanotube Conjugates for Tissue-Translatable Glucose Nanosensors

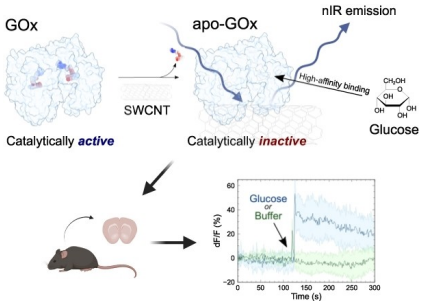

This paper presents the development of nIR fluorescent single-walled carbon nanotube (SWCNT) based nanosensors for glucose imaging. The authors find that the fluorescence modulation of GOx-SWCNT is not associated with the enzymatic activity but rather triggered by the substrate-enzyme binding. Leveraging this unique mechanism, the authors developed catalytically inactive nanosensors that enable glucose imaging in mouse brain slices.